IEEE Access
Multidisciplinary | Rapid Review | Open Access Journal

Received July 20, 2018, accepted September 3, 2018, date of publication September 17, 2018, date of current version October 12, 2018.

Digital Object Identifier 10.1109/ACCESS.2018.2870757

On the Coexistence of LTE-LAA in the Unlicensed Band: Modeling and Performance Analysis

NAIM BITAR[1], (Student Member, IEEE), MOHAMAD OMAR AL KALAA[2], (Member, IEEE), SETH J. SEIDMAN[2], (Member, IEEE), AND HAZEM H. REFAI[1], (Member, IEEE)

[1]Department of Electrical and Computer Engineering, The University of Oklahoma, Tulsa, OK 74135, USA
[2]Center for Devices and Radiological Health, U.S. Food and Drug Administration, Silver Spring, MD 20993, USA

Corresponding author: Naim Bitar (naimbitar@ou.edu)

This work was supported in part by an appointment to the Internship/Research Participation Program at the U.S. Food and Drug Administration, administered by the Oak Ridge Institute for Science and Education through an inter-agency agreement between the U.S. Department of Energy and the FDA.

ABSTRACT Long term evolution (LTE) technology leveraging the unlicensed band is anticipated to provide a solution for the challenges stemming from the rapid growth of mobile wireless services, the scarcity of available licensed spectrum, and the expected significant increase in mobile data traffic. Ensuring fair operation in terms of spectrum sharing with current unlicensed spectrum incumbents is a key concern relative to the success and viability of Unlicensed LTE (U-LTE). This paper addresses the problem of modeling and evaluating the coexistence of LTE license-assisted-access in the unlicensed band. The paper presents a novel analytical model using Markov chain to accurately model the LAA listen-before-talk scheme, as specified in the final technical specification 36.213 of 3GPP release 13 and 14. Furthermore, model validation is demonstrated through numerical and simulation results comparison. Model performance evaluation is examined and contrasted with IEEE 802.11 distributed coordination function. Finally, a comprehensive coexistence performance analysis is conducted for both homogeneous and heterogeneous network scenarios and coexistence results are presented and discussed herein.

INDEX TERMS LBT, LTE-LAA, LTE-U, LTE unlicensed, LWA, Markov chain, multefire.

I. INTRODUCTION

The amount of data traffic carried over cellular networks is expected to significantly increase in the coming years [1]. Moreover, the growing number of wireless devices accessing an increasing number and variety of demanding services magnifies this challenge several folds. Consequently, high capacity networks and service provisioning of very high data rates has become an essential requisite for meeting customers' expectations in a wide range of applications used in diverse environments including residential, professional, and healthcare environments. More spectrum is therefore needed for cellular operators to meet this increasing demand. Unlicensed Long-Term Evolution (U-LTE) is a candidate solution that is anticipated to address these aforementioned challenges. Insuring fair operation in terms of spectrum sharing with unlicensed spectrum incumbents has proven to be a challenging and critical mandate for the success of U-LTE. To address this issue, a number of mechanisms have been developed to modify LTE and make it more amenable to coexist with other wireless technologies (e.g., LTE Unlicensed (LTE-U), Licensed-Assisted-Access (LAA), enhanced-LAA (eLAA), LTE-WLAN Aggregation (LWA) and Multefire). During their development, initial experimentation assessed effects on the performance of 802.11 incumbent wireless networks utilizing the same unlicensed band and primarily carried out by commercial operators. Minor impact was indicated [2]–[5]. Other experiments conducted by the research community, demonstrated that Wireless Fidelity (Wi-Fi) performance would be seriously affected, all while LTE performance would be only slightly degraded [6]–[8]. Such discordant outcome could be attributed to discrepancies in experimentation tools used to implement LTE unlicensed specifications. Furthermore, simulations and/or empirical experiment results remain independently unverifiable, as they rely on proprietary tools and resources. Consequently, it is imperative that an analytical framework is utilized for analyzing and evaluating proposed specifications. Having this will allow accurate transparent analytical assessment of the underlying mechanisms while eliminating implementation biases that could arise in empirical experimentation. This paper builds upon this framework addressing the issue of evaluating and modeling LTE-LAA's Listen-Before-Talk (LBT) mechanism and its effect on coexistence in the unlicensed band. Initially, our work reviewed the coexistence mechanism standardized for LTE-LAA in the 3rd Generation Partnership Project (3GPP) release 13 and 14. Then, a novel analytical model using Markov Chain to accurately model the LAA LBT mechanism is presented. After that, model validation is subsequently demonstrated through numerical and simulation results comparison. Performance evaluation between the LAA-LBT and the Institute of Electrical and Electronics Engineers (IEEE) 802.11 Distributed Coordination Function (DCF) is conducted. In addition, a comprehensive coexistence analysis of homogeneous and heterogeneous network scenarios involving LTE-LAA Evolved Node Bs (eNB) and Wi-Fi Access Points (AP) is carried out. Results are presented and discussed herein.

This work contributes to our field in three significant areas. 1) The paper establishes an accurate analytical model that facilitates numerical analysis of the LTE-LAA coexistence mechanism as indicated in the final standardized frozen technical specification (TS) 36.213 of 3GPP release 13 and 14. 2) The paper expounds the LTE-LAA LBT and delineates the effects of the proposed coexistence mechanism and its parameters through extensive analysis. 3) The paper details a comprehensive coexistence analysis, conducted for both homogeneous and heterogeneous networks, clearly identifying use cases where the LTE-LAA LBT mechanism obtains increased gain over co-channel incumbents and the effects on both co-channel and co-located networks. The outcome of this work provides an unequivocal and clear understanding of the implications and effects LTE-LAA LBT has on network coexistence performance. The balance of this paper is organized as follows: The following section presents the background and related work exposition on LTE-LAA coexistence in the unlicensed band. Section 3 reviews the coexistence mechanism standardized for LTE-LAA in 3GPP release 13 and 14. Section 4 presents the proposed analytical model of LTE-LAA LBT. Section 5 demonstrates validation work through numerical and simulation analysis and demonstrates performance evaluation of LAA-LBT by means of the proposed model contrasted with 802.11 DCF. Section 6 presents a comprehensive coexistence analysis of both homogeneous and heterogeneous network operations. Finally, section 7 concludes this paper.

II. BACKGROUND AND RELATED WORK

With the initial consideration of permitting licensed LTE to supplement its downlink with unlicensed spectrum, various experimentations indicated LTE would unfairly occupy the unlicensed-band and induce adverse effects on current unlicensed-band occupants [9]–[11]. This impelled research to ensue in an attempt to address this challenge. However, with two distinct global-market regulatory constraints i.e. (some regions with no LBT restriction, and others requiring LBT), two research directions developed, namely LTE-U and LTE-LAA. The first assumes no LBT constraint and is currently adopted by the LTE-U Forum [12]. The approach can readily apply 3GPP release 10, 11 and 12 enhancements coupling them with coexistence methods for monitoring band occupancy and attempting to replicate channel retention/idle time in their resource allocation mechanisms through duty cycling [13]. The second approach has been standardized in 3GPP release 13, includes LBT as a core mandate and was further enhanced in 3GPP release 14 to support uplink operation. Recently, techniques to improve the LBT procedure for LTE-LAA has been a very active research area. LBT provides coexistence by enabling channel sensing and dynamic spectrum access as recommended by 3GPP for unlicensed operation. Initial considerations for LAA examined adopting 802.11's DCF founded on Carrier Sense Multiple Access/Collision Avoidance (CSMA/CA) as basis for LTE-LAA coexistence. However, the drawbacks of not fully exploiting the enhancements of LTE for improved spectral efficiency, low network overhead, and high throughput motivated the consideration of an enhanced approach. Consequently, solutions employed Wi-Fi's DCF scheme while implementing suitable optimization to its parameters. Reference [14] proposed a smaller contention window (CW) size for LAA nodes to ensure higher spectrum access probability, less spectral access delay, and higher throughput. Reference [15] optimized the CW size to maximize total throughput of a heterogeneous LTE and Wi-Fi network. Reference [16] proposed a fixed CW for a given data rate and multi-stage back-off scheme to facilitate collision avoidance. However, in all aforementioned implementations, LTE attained an unfair advantage over Wi-Fi, whose performance decreased as the number of LTE nodes sharing the same spectrum increased. An adaptive, adjusted CW was proposed in [17] and was based on available licensed bandwidth and traffic generated by the Wi-Fi network, presuming stations exchange traffic load information. Research in [18]–[21] also proposed an adaptive CW with the goal of optimizing channel occupancy. The authors adjusted the Transmission Opportunity (TXOP) duration of LTE nodes according to Wi-Fi activity, cell load, channel condition, and transmission latency. Although few papers in the associated literature proposed a solution aberrant of DCF, some report on the interference caused by LTE-LAA. For example, [22] proposed adaptive power and bandwidth adjustment to guarantee fair coexistence between a standalone LTE system and Wi-Fi. Bhorkar *et al.* [23] proposed a modified Medium Access Control (MAC) protocol for LAA co-existence. In this protocol, a CSMA like LBT technique for LAA in synchronous mode and asynchronous mode was proposed. Reference [24] exploited frequency reuse between neighboring LAA nodes for reducing interference and allowing the systems to coexist. Finally, [25] proposed dynamically switching between traffic offloading and resource sharing schemes, transferring Wi-Fi users to LAA to relinquish some unlicensed resources. The body of this research work guided the development of the 3GPP study item published in 2015, widely known as technical report 36.889 [26]. This report was the first official document to specify LTE-LAA's operation and has been the basis of research material assessing LTE-LAA performance [27]–[30]. Technical report 36.889 defines two operation modes: 1) LBT without random backoff (frame-based LBT) which utilizes a fixed CW window, and 2) LBT with a binary exponential CW random backoff (load-based LBT), which is identical to 802.11's DCF for coexisting with other incumbents in the unlicensed band [30]. Notably, the final "frozen" release 13 3GPP standard specification of TS 36.213 [31], redefined the coexistence mechanism of LTE-LAA. By adopting only the load-based LBT mechanism and introducing a new operation parameter, (i.e. K parameter described fully in the subsequent section), LAA's LBT is no longer identical to Wi-Fi's DCF, and instead is described to "fundamentally resemble" Wi-Fi's DCF in the final specification. This modification has not been addressed in research work aiming to model the coexistence performance of LTE-LAA [8], [29], [32]–[38]. Prior analytical models for Wi-Fi and LTE-LAA coexistence developed in [15] and [16] are similar in the aptitude and essence of this work. In [16], channel access and success probability are evaluated for LTE-LAA and Wi-Fi coexistence with a simplified version of CSMA employed in Wi-Fi by considering no exponential backoff and a fixed contention window size. In [15], the coexistence of LTE-LAA and Wi-Fi throughput is evaluated according to the aforementioned 3GPP technical report TR 33.889 [26] (again does not conform to the final 3GPP release 13 standard specification of TS 36.213). In summary, a proper evaluation of Wi-Fi and LTE-LAA LBT coexistence as standardized by 3GPP [31] is still outstanding. Finally, at the time of compiling this work a non-peer reviewed paper [39] has been uploaded to arXiv.org e-Print archive, which confirms the lack in LTE-LAA literature. The authors note that their analysis does not investigate fair sharing of coexistence which is evident in their use of technology specific data rates in their expressions and analysis work. This deficiency creates an imbalance in actual channel usage time, and results in imprecise interpretation of coexistence fairness. Furthermore, authors assume that Wi-Fi's maximum contention stage occurs for only one additional retransmission which does not conform to the Wi-Fi standard [40]. The paper does not consider inter-network transmission in their expressions for probability of successful transmission, and authors do not investigate homogeneous network coexistence. Thereupon, the work detailed in this paper aims to fill this gap. Our work delineates the key fundamental difference between Wi-Fi's DCF and LTE-LAA LBT as described in the final specification of LTE-LAA TS 36.123. To the best of our knowledge, our work establishes the first accurate analytical model that allows numerical analysis of the coexistence mechanism of LTE-LAA as found in the final standardized frozen technical specification (TS) 36.213 of 3GPP release 13 and 14. This work expounds the LTE-LAA LBT and delineates the effects of the proposed coexistence mechanism and its parameters through extensive analysis. Finally, our work details a comprehensive coexistence analysis, conducted for both homogeneous and heterogeneous networks. The outcome of this work gives a detailed description of the implications and effects the standardized LTE-LAA LBT mechanism has on the coexistence performance of the network.

III. LTE-LAA

LTE-LAA is the 3GPP standardized mechanism developed for deploying LTE in the unlicensed band. It was standardized by 3GPP in Release 13, and later enhanced in 3GPP Release 14 (eLAA) to support uplink operation. LTE-LAA is the first standardized mechanism that supports both downlink (DL) and uplink (UL) transmissions and employs LBT as the primary coexistence mechanism. Carrier aggregation with at least one Secondary Cell (SCell) has been specified, with operation limited to the globally available 5 GHz unlicensed spectrum. 3GPP release 13 defines two technical reports (TR 36.889 [26] & TR 36.789 [41]) and six technical specifications (TS 36.300 [42], TS 36.211 [43], TS 36.104 [44], TS 36.141 [45], TS 36.133 [46] & TS 36.213 [31]) that collectively standardize LTE-LAA. A brief description of each follows: **TS 36.300** [42] gives an overall description of the release Evolved Universal Terrestrial Radio Access (E-UTRA) and Evolved Universal Terrestrial Radio Access Network (E-UTRAN) which define the radio operational aspects of LAA. **TR 36.889** [26] is the initial study item on LAA to the unlicensed spectrum. This report specifies regulatory requirements for the unlicensed band per region, an LAA carrier aggregation feasibility study, deployment scenarios for LAA, design targets and functionalities and finally coexistence evaluations and results. **TR 36.789** [41] specifies the evaluation methodology for multi-node coexistence. This technical report explains how to conduct multi-node tests involving two Rel-13 LAA BSs or one Rel-13 LAA BS and one other wireless system, e.g. IEEE 802.11 system to make sure that the two systems can co-exist in the same unlicensed spectrum. **TS 36.211** [43] chapter 4 defines a new frame structure type 3 applicable to LAA secondary cell operation with normal cyclic prefix. **TS 36.104** [44] specifies carrier aggregation of component carriers in different operating bands. Chapter 9 presents channel access parameters for LTE-LAA. **TS 36.141** [45] chapter 9 specifies eNB conformance testing procedures for LBT. Conformance testing is used to verify the accuracy of the energy detection threshold, Maximum Channel Occupancy Time (MCOT) and minimum idle time under normal operating conditions in regards to LAA operation. **TS 36.133** [46] specifies requirements for support of radio resource management for LAA under frame structure 3. **TS 36.213** [31] chapter 15 defines the channel access procedure and LBT mechanism for LAA. Release 13 targets LAA to be a global solution framework that achieves effective and fair coexistence with Wi-Fi and adjacent LAA networks deployed by different operators. Accordingly, LAA supports: 1) LBT, 2) Discontinuous transmission on a carrier with limited maximum transmission duration, 3) Dynamic frequency and carrier selection, 4) Transmit power control and 5) Radio Resource Management (RRM) measurements.

TABLE 1. Channel access priority class for DL.

Priority Class (p)	m_p	$CW_{min,p}$	$CW_{max,p}$	$T_{mcot,p}$	allowed CW_p sizes
1	1	3	7	2 ms	3,7
2	1	7	15	3 ms	7,15
3	3	15	63	8 or 10 ms	15,31,63
4	7	15	1023	8 or 10 ms	15,31,63,127, 255,511,1023

TABLE 2. Mapping between channel access priority classes and QCI.

Channel Access Priority Class	QCI
1	1, 3, 5, 65, 66, 69, 70
2	2, 7
3	4, 6, 8, 9
4	-

A. LAA-LISTEN BEFORE TALK

LAA applies LBT before transmitting on a SCell. The transmitter senses the channel to determine whether the channel is free or busy. If the channel is determined to be free, transmission may occur. Therefore in LTE-LAA, the configured set of serving cells for a User Equipment (UE) always include at least one SCell operating in the unlicensed spectrum. For downlink LAA, four Channel Access Priority Classes (CAPCs) are defined [31] shown in table 1. The smaller the LBT priority class number, the higher the priority. CAPCs are assigned based on traffic type and are mapped to different standardized Qos Class Indicators (QCIs) [47] as shown in table 2. LAA mandates that after a successful LBT, if a DL burst within a Physical Downlink Shared Channel (PDSCH) is transmitted, the transmission duration shall not exceed the MCOT per CAPC denoted $T_{mcot,p}$. The defer duration T_d, which is the minimum time a node has to wait after the channel becomes idle, is equal to a fixed duration $T_f = 16\mu s$, plus (m_p) consecutive number of time-slot durations $T_{sl} = 9\mu s$ which are identical to Wi-Fi's time-slot. Minimum contention window size, $CW_{min,p}$ and maximum contention window size $CW_{max,p}$ per priority class along with all the aforementioned parameters are shown in table 1. For $p = 3$ and $p = 4$, if the absence of any other technology sharing the carrier can be guaranteed on a long term basis (e.g. by level of regulation), $T_{mcot,p} = 10ms$, otherwise, $T_{mcot,p} = 8ms$. The LBT mechanism of LTE-LAA is said to fundamentally resemble the CSMA/CA of a 802.11. Before transmitting, the eNB performs Clear Channel Assessment (CCA) using energy detection. The equipment observes the operating channel for the duration of T_d. The operating channel is considered occupied if the energy level in the channel exceeds a threshold X_{Th} during any slots of the duration T_d. If the equipment finds the channel to be clear, and the backoff counter N is equal to zero, it may transmit immediately. If the equipment finds an operating channel occupied, it must not transmit, and instead it must perform an Extended CCA (ECCA) check in which the operating channel is observed for a random duration. Algorithm 1 delineates a pseudo-code representing the LTE-LAA LBT mechanism.

Algorithm 1 LAA LBT Mechanism

global variables
  $N = N_{init} \in [0, CW_p]$ random uniform back-off counter.
end global variables
procedure LBT
CCA:
  for $T_d = T_f + (m_p \cdot T_{sl})\mu s$ **do** sense channel
    if Energy detected $< X_{Th}$ **then**
      Check Backoff counter N:
      if $N == 0$ **then**
        Transmit
      else
        goto *ECCA Step 3)*
    else
      goto *ECAA Step 1)*
ECCA:
  Step1):
    Generate $N = N_{init}$
    Go to step 4)
  Step2):
    for $T_d = T_f + (m_p \cdot T_{sl})\mu s$ **do** sense channel
      if Energy detected $< X_{Th}$ **then**
        goto *ECCA Step 3)*
      else
        goto *ECCA Step 2)*
  Step3):
    for $T_{sl} = 9\mu s$ **do** sense channel
      if Energy detected $< X_{Th}$ **then**
        $N = N - 1$
        goto *ECCA Step 4)*
      else
        goto *ECCA Step 2)*
  Step4):
    if $N == 0$ **then**
      Transmit
    else
      goto *ECCA Step 3)*

B. CONTENTION WINDOW ADJUSTMENT

The CW is adjusted based on the Hybrid Automatic Repeat Request (HARQ) Acknowledgment (ACK) feedback. HARQ-ACK feedback can take a value from ACK, Negative Acknowledgment (NACK), and Discontinuous Transmission (DTX). ACK refers to the situation of correct reception, NACK refers to the situation where control information (i.e., Physical Downlink Control Channel (PDCCH)) is correctly detected but there is an error in the data (i.e., PDSCH) reception, and DTX refers to the situation when a UE misses the control message containing scheduling information (i.e., PDCCH), rather than the data itself (i.e., PDSCH). No HARQ-ACK feedback and DTX are considered as NACK. Furthermore, bundled HARQ-ACK across (x) subframes are considered as (x) HARQ-ACK responses.

Accordingly, CW_p is adjusted in a similar manner to Wi-Fi DCF. Setting $CW_p = CW_{min,p}$ according to the traffic priority class, when at least four fifths of all HARQ-ACK values corresponding to PDSCH transmission(s) in the reference subframe are NACK, CW_p is increased to the next higher allowed value for that specific priority class according to table 1. This corresponds to increasing the backoff stage for retransmissions. The key difference between Wi-Fi and LAA, found in the contention window adjustment procedure, occurs when the contention window size CW_p reaches the maximum value allowed CW_{max}. In Wi-Fi this value is retained as long as collisions continually occur in re-transmissions [40]. Once a certain number of re-transmissions have been attempted (lifetime of a packet) and if packet collision occurs, the transmitted packet is discarded. In contrast, LAA-LBT specifies a K parameter value in the standard. This value is set by each operator and ranges between 1 and 8. It dictates how many times CW_{max} may be used. Once K re-transmissions have been attempted, LAA-LBT resets CW_p to CW_{min} and re-transmission continues again from the lowest stage. Here lies the fundamental difference between both coexistence mechanisms.

IV. LTE-LAA PROPOSED MARKOV-CHAIN MODEL

Consistent with previous work in [15], [16], [48], and [49], our analysis and proposed analytical model adopt: 1) a saturated traffic model where all the nodes always have packets to transmit, and 2) an ideal channel where the Bit Error Rate (BER) is 0. Accordingly, we assume P_l to be the probability of an LAA packet collision occurring. Also, we assume that packet collision is constant and independent and the reference subframe is the starting subframe of the most recent transmission on the carrier made by the eNB, for which at least some HARQ-ACK feedback is expected to be available. Under saturation conditions, the probability that all HARQ-ACK values corresponding to PDSCH transmission(s) in the reference subframe are NACK can be given by $\gamma = P_l$. Let φ be the probability that K re-transmissions at CW_{max} have occurred, then $\varphi = \gamma^{K-1}$. Let i represent the back-off stage, $W_i = 2^i \times W$ for i ∈ $[0, 1, \ldots m]$ the contention window, and r represents the back-off chosen value. W is the minimum contention window (CW_{min}). We now draw the 2D Markov Chain depicting the operation of LAA-LBT contention window adjustment as shown in figure 1. A glossary of variables used in the development and analysis of this model are presented in table 3.

A. ONE-STEP TRANSITION PROBABILITIES

Calculating the one-step transition probabilities of the Markov Chain of figure 1 we find:

$$p(i, r|i, r+1) = 1 : \quad i \in [0, m], \; r \in [0, W_i - 2],$$

$$p(0, r|i, 0) = \frac{(1-\gamma)}{W_0} : \quad i \in [0, m-1], \; r \in [0, W_i - 1],$$

$$p(i, r|i-1, 0) = \frac{\gamma}{W_i} : \quad i \in [1, m], \; r \in [0, W_i - 1],$$

TABLE 3. Glossary of variables.

Abbreviation	Definition
p	Priority Class ∈ [1,2,3,4]
m_p	Number of backoff stages for priority class p
CW_{min} , W	Minimum contention window size
CW_{max}	Maximum contention window size
$T_{mcot,p}$	Maximum channel occupancy for priority class p
T_d	Transmission differ duration for LAA eNB
T_{sl}	LAA timeslot duration
T_f	Fixed time duration =16μs
X_{Th}	Energy detection threshold
N	Backoff counter
γ	Probability of LAA transmission burst collision
i	Contention window stage
r	Backoff value chosen
W_i	Contention window size for stage i
$b_{i,r}$	Stationary probability for stage i, backoff value r
m	Maximum backoff stage
τ_l	Probability of transmission for LAA
τ_w	Probability of transmission for Wi-Fi
b_r	Bitrate
γ	Propagation Delay
ACK	Acknowledgment size
$DIFS$	Distributed Interframe Space
$SIFS$	Short Interframe Space
$\sigma = T_{sl}$	Wi-Fi Timeslot duration
P_w	Collision Probability for heterogenous Wi-Fi
P_l	Collision Probability for heterogenous LAA
P_{trw}	Trans. Probability for heterogenous Wi-Fi
P_{trl}	Trans. Probability for heterogenous LAA
P_{sl}	Successful Trans. Probability for heterogenous LAA
P_{sw}	Successful Trans. Probability for heterogenous Wi-Fi
T_{ws}	Time due to successful heterogenous Wi-Fi transmission
T_{ls}	Time due to successful heterogenous LAA transmission
T_{wc}	Time due to collision heterogenous Wi-Fi transmission
T_{lc}	Time due to collision heterogenous LAA transmission
T_a	Time due inter-network transmission

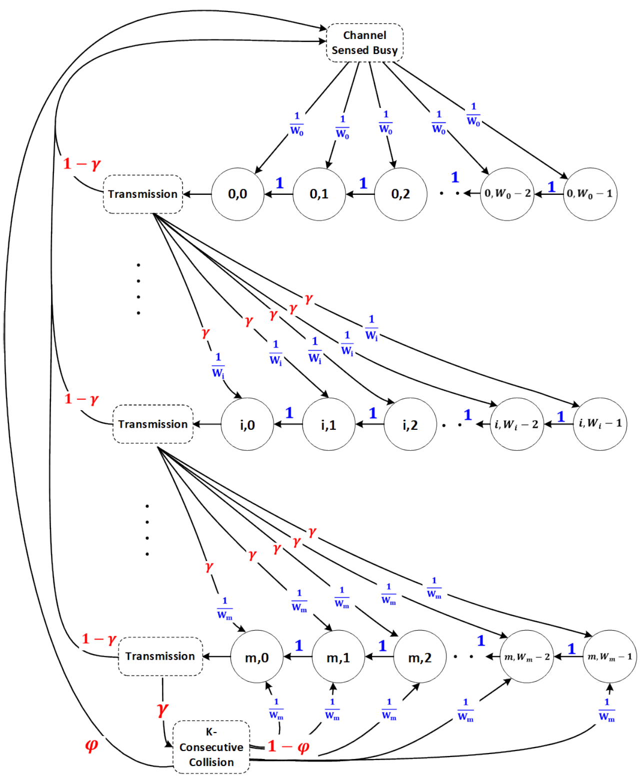

FIGURE 1. Proposed LAA-LBT Markov chain.

$$p(m, r|m, 0) = \frac{\gamma - \gamma^K}{W_m} : \quad r \in [0, W_m - 1],$$

$$p(0, r|m, 0) = \frac{\gamma^K - \gamma + 1}{W_0} : \quad r \in [0, W_0 - 1].$$

B. STATIONARY PROBABILITIES

Let $b_{i,r} = lim_{t\to\infty} p\{i,r\}$, we find: When $i = 0$ and $r \in [1, W_0 - 1]$:

$$b_{i,r} = \frac{W_i - r}{W_i} \cdot \Big(\sum_{j=0}^{m-1} b_{j,0} \cdot (1-\gamma) + b_{m,0} \cdot (\gamma^K - \gamma + 1)\Big). \tag{1}$$

When $i \in [1, m-1]$ and $r \in [1, W_i - 1]$ we find:

$$b_{i,r} = \frac{W_i - r}{W_i} \cdot b_{i-1,0} \cdot \gamma. \tag{2}$$

When $i = m$ and $r \in [1, W_m - 1]$ we find:

$$b_{i,r} = \frac{W_i - r}{W_i} \cdot \Big(b_{i-1,0} \cdot \gamma + b_{i,0} \cdot (\gamma - \gamma^K)\Big). \tag{3}$$

When $0 < i < m$ and $r = 0$,

$$b_{i,0} = \gamma^i \cdot b_{00}. \tag{4}$$

For $i = m$, $r = 0$:

$$b_{m,0} = b_{m-1,0} \cdot \gamma + b_{m,0} \cdot (\gamma - \gamma^K)$$
$$b_{m,0} \cdot (1 - \gamma + \gamma^K) = b_{m-1,0} \cdot \gamma$$

Using equation (4) we find the stationary probability to be:

$$b_{m,0} = \frac{\gamma^m}{\gamma^K - \gamma + 1} \cdot b_{0,0}. \tag{5}$$

Using the geometric series we find the sum found in equation (1) to be,

$$\sum_{j=0}^{m-1} b_{j,0} = b_{0,0} \cdot \frac{1-\gamma^m}{1-\gamma}. \tag{6}$$

We now use equations (4), (5) and (6) to summarize and express (1), (2) and (3) as (7):

$$b_{i,r} = \frac{W_i - r}{W_i} \cdot b_{i,0} : \quad i \in [0, m],\ r \in [0, W_i - 1] \tag{7}$$

By imposing the normalizing condition:

$$\begin{aligned}
1 &= \sum_{i=0}^{m}\sum_{r=0}^{W_i-1} b_{i,r} = \sum_{i=0}^{m}\sum_{r=0}^{W_i-1} \frac{W_i - r}{W_i} \cdot b_{i,0} \\
&= \sum_{i=0}^{m} b_{i,0} \cdot \Big(\frac{W_i+1}{2}\Big) \\
&= \frac{1}{2}\sum_{i=0}^{m} (b_{i,0} \cdot W_i + b_{i,0}) \\
&= \frac{1}{2}\Big[\sum_{i=0}^{m} b_{i,0} \cdot 2^i W + \sum_{i=0}^{m} b_{i,0}\Big] \\
&= \frac{1}{2}\Big[\sum_{i=0}^{m-1} (b_{i,0} \cdot 2^i W) + b_{m,0} \cdot 2^m W + \sum_{i=0}^{m-1} b_{i,0} + b_{m,0}\Big] \\
&= \frac{b_{0,0}}{2}\Big[\sum_{i=0}^{m-1} (2\gamma)^i \cdot W + \frac{(2\gamma)^m}{\gamma^K - \gamma + 1} \cdot W \\
&\quad + \frac{1-\gamma^m}{1-\gamma} + \frac{\gamma^m}{\gamma^K - \gamma + 1}\Big] \\
&= \frac{b_{0,0}}{2} \cdot \Big[\frac{(1-\gamma)(1 + W \cdot (2\gamma)^m) + \gamma^K (1-\gamma^m)}{(1-\gamma)(\gamma^K - \gamma + 1)} \\
&\quad + \frac{W(1-(2\gamma)^m)}{1-(2\gamma)}\Big]
\end{aligned} \tag{8}$$

Solving (8) we find $b_{0,0}$.

$$b_{0,0} = \frac{X}{Y} \tag{9}$$

Where,

$$\begin{aligned}
X &= 2 \cdot (1-\gamma)(\gamma^K - \gamma + 1)(1-(2\gamma)), \\
Y &= (1-\gamma)(1-2\gamma)(1+W(2\gamma)^m) + \gamma^K (1-\gamma^m)(1-2\gamma) \\
&\quad + W(1-(2\gamma)^m)(1-\gamma)(\gamma^K - \gamma + 1)
\end{aligned}$$

We now express the probability of an LAA node transmitting, denoted τ_l, as:

$$\begin{aligned}
\tau_l &= \sum_{i=0}^{m} b_{i,0} = \sum_{i=0}^{m-1} b_{i,0} + b_{m,0} \\
&= b_{0,0} \cdot \Big(\frac{\gamma^K - \gamma + 1 - \gamma^{m+K}}{(1-\gamma) \cdot (\gamma^K - \gamma + 1)}\Big)
\end{aligned} \tag{10}$$

Using (9) in (10) we find:

$$\tau_l = \frac{A}{B + C + D} \tag{11}$$

where:

$$\begin{aligned}
A &= 2 \cdot (1-2\gamma) \cdot (\gamma^K - \gamma + 1 - \gamma^{m+K}) \\
B &= (1-\gamma) \cdot (1-2\gamma) \cdot (1 + W(2\gamma)^m) \\
C &= \gamma^K \cdot (1-\gamma^m) \cdot (1-2\gamma) \\
D &= W \cdot (1-(2\gamma)^m) \cdot (1-\gamma) \cdot (\gamma^K - \gamma + 1)
\end{aligned}$$

Recall W refers to the minimum contention window size allowed (W_{min}). We note that when $m = 0$ i.e. (No exponential backoff is considered) the probability of transmission in (11) simplifies to: $\tau_l = \frac{2}{W+1}$ matching the probability of transmission for 802.11 as found in [48].

V. MODEL VALIDATION

To validate the accuracy of the proposed model, we compare the numerical results obtained using the analytical model with simulation results in terms of the normalized saturation throughput. For this, we consider a network of n neighboring stations utilizing the LTE-LAA LBT mechanism. The probability γ, that any single transmission of a BS encounters a collision, is the probability that in a time slot, at least one of the $n-1$ remaining stations transmit. i.e.

$$\gamma = 1 - (1 - \tau_l)^{n-1} \tag{12}$$

Solving the non-linear system of (11) and (12) using numerical techniques yields γ and τ_l. We define the normalized system throughput S, as the fraction of time the channel is

TABLE 4. Channel access parameters.

Parameter	Unit
p: Priority Class	p = 4
m_p	7
CW_p: Allowed sizes	[15,31,63,127,255,511,1023]
$T_{mcot,p}$: Maximum channel occupancy time	8ms
EP: Packet Payload	8184 bits
b_r: bitrate	1Mbps
δ: Propagation Delay	$1\mu s$
H: Packet Header (PHY + MAC)	400bits
ACK: HARQ-ACK	240bits
σ: TimeSlot	$9\mu s$
DIFS: $16\mu s + (m_p + \sigma)$	$79\mu s$
SIFS	$16\mu s$

used to successfully transmit payload bits. This can be given as:

$$S = \frac{P_s P_{tr} EP}{(1 - P_{tr})\sigma + P_{tr} P_s T_s + P_{tr}(1 - P_s)T_c}. \quad (13)$$

Where $P_{tr} = 1 - (1 - \tau_l)^n$ is the probability of at least one transmission occurring in the considered time slot, $P_s = \frac{n\tau_L(1-\tau_L)^{n-1}}{P_{tr}}$ is the probability of a successful transmission, σ is the time slot duration. $EP = T_{mcot,p}$. T_s and T_c were fixed for both numerical and simulation analysis at 8.9ms and 8.7ms respectively according to LAA channel access priority class $P = 4$. Numerical results were computed using Matlab by solving (11) and (12) with the parameters taken from Table 4. Simulation of LAA-LBT procedure was done in a simulator built in Python that ran for n contending stations for 10^8 time steps utilizing the same parameters. The simulation starts with all n nodes attempting to transmit and consequently backing off according to the standard defined in LTE-LAA LBT mechanism. Each node maintains backoff value, backoff stage, and re-transmission counter that are updated upon successful transmission or collision. Transmission, collision, and idle times are tracked to estimate S as an average of x simulation runs. This was repeated for maximum back-off stages $m = [2, 4, 6]$ and LAA-LBT parameter $K = 1$. Figure 2 depicts a comparison plot between both numerical and simulated saturation throughput results attained. Calculating the Root Mean Squared Error (RMSE) between the two yields a value of 0.0045. This signifies high model accuracy.

A. LTE-LAA LBT VS. WI-FI LBT PERFORMANCE ANALYSIS

Model performance analysis followed contrasting the standardized LAA-LBT τ_l developed above and Wi-Fi's LBT with a transmission probability τ_w given in [48] as:

$$\tau_w = \frac{2(1 - 2P_w)}{(1 - 2P_w)(W + 1) + p_w W(1 - (2p_w)^m)}. \quad (14)$$

The objective of the analysis in this subsection is to clearly delineate the performance difference between the LBT mechanisms of LAA and Wi-Fi distinctly. This allows us to gain a deeper and more clear understanding of what effect the K parameter has on the performance of LTE-LAA LBT. To achieve this, we set $T_c = (H + EP)/b_r + DIFS + \delta$ and $T_s = (H + EP)/b_r + SIFS + \delta + ACK + DIFS + \delta$

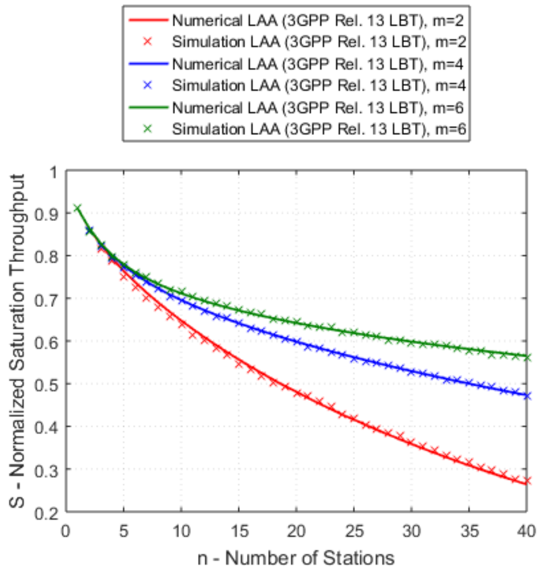

FIGURE 2. Simulation vs. numerical analysis results.

calculated from table 4, for both networks. We observe in figure 3, as the number of n co-channel LAA stations operating LAA-LBT increases, the saturation throughput drops below than that of n co-channel Wi-Fi APs operating Wi-Fi's LBT. This is confirmed in figure 4 where we can observe that LTE-LAA LBT achieves higher probability of transmission with an increasing number of contending nodes. This can be explained as follows: as the number of nodes increases, collision increases as well, resulting in higher backoff stages. As LAA-LBT resets CW_p once the maximum backoff stage retransmission has been reached $K = 1$ times, the lower stage will increase transmission probability, which in turn will cause more collisions and reduce throughput. However, this phenomenon only occurs when all n contending nodes are using the same LAA-LBT mechanism. Thus, it can be concluded that a dense homogeneous network consisting of LAA-LTE stations operating the standardized LBT mechanism experiences increased collisions. However, an LAA-LTE node stands to gain an advantage when it finds itself amongst n contending Wi-Fi nodes due to the increased transmission probability it solely gains. This is further evident in figure 3 which demonstrates that by increasing the value of $K = [1, 2, 4, 5, 8, 16]$, the probability of transmission decreases and the saturation throughput increases until it approaches Wi-Fi LBT throughput at around $K = 16$ to a negligible difference. It is noted however, that $K = 8$ is the maximum permitted value in the specification. In essence, the K parameter added in the final specification provides an LTE-LAA eNB operator with the agility to coexist in both homogeneous and heterogeneous networks. By setting K=1, the LAA eNB benefits from an increased probability of transmission over co-channel neighboring Wi-Fi stations (heterogeneous network operation). Setting K=8 prevents co-channel collocated eNBs (homogeneous network operation) from degrading throughput. Finally, plotting the initial

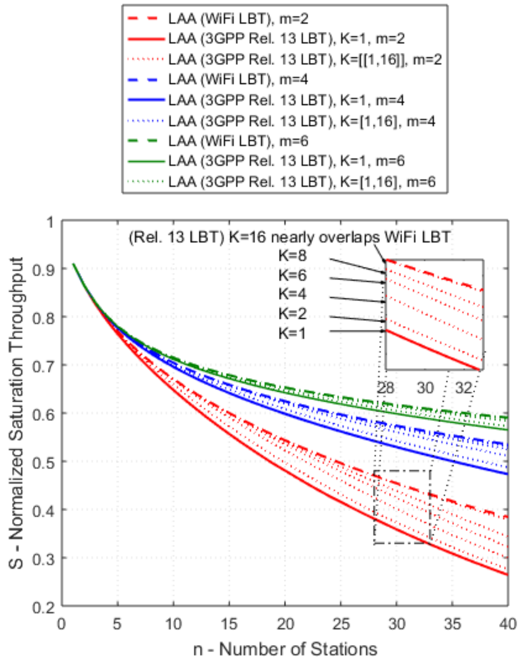

FIGURE 3. Normalized saturation throughput for $K \in [1, 2, 4, 6, 8, 16]$.

contention window size vs. normalized saturation throughout, we observe in figure 5 that dense LAA networks are increasingly affected by the K parameter setting. Moreover, we observe that the initial contention window size has a significant effect on the LTE-LAA LBT performance. We also observe that there exists an optimal contention window size for yielding maximum saturation throughput. Therefore, LAA stations utilizing the standardized LBT mechanism can achieve considerable performance gain by passively detecting the number of co-channel operating nodes and optimizing the initial contention window size along with the K parameter setting.

VI. HOMOGENEOUS AND HETEROGENEOUS COEXISTENCE PERFORMANCE ANALYSIS

In this section we evaluate the coexistence performance for both homogenous and heterogenous network scenarios for the standardized LTE-LAA LBT mechanism. We first derive probability expressions for heterogeneous network operation, then utilizing previously dervied homogenous expressions along with the heterogenous expressions, we conduct our analysis. In this, we assume the heterogeneous network consists of n_w Wi-Fi APs and n_l LTE-LAA eNBs which are co-channeling and co-located, each with a full buffer. We consider only the DL transmission for one client per AP/eNB, implying the contention is between only the APs and eNBs. τ_w and τ_l denote the transmission probability of Wi-Fi and LTE-LAA respectively.

From (11) we employ the derived transmission probability for LTE-LAA, and from (14) we obtain the probability of transmission for Wi-Fi. Accordingly, for the network consisting

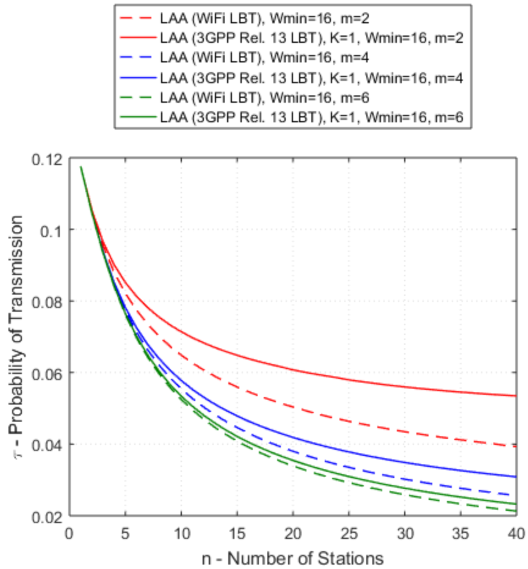

FIGURE 4. LAA vs. Wi-Fi probability of transmissions (homogeneous network).

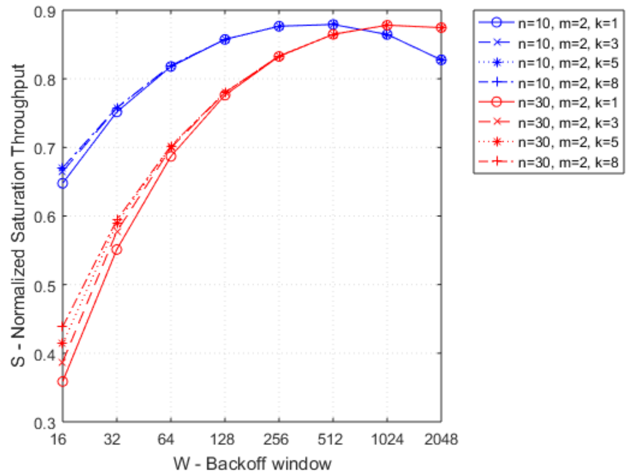

FIGURE 5. Normalized saturation throughput vs. initial contention window size.

of n_w APs and n_l eNBs, the collision probability of a Wi-Fi AP transmitting with at least one of the other remaining $(n_w - 1)$ APs and n_l eNB stations can be given as:

$$P_w = 1 - (1 - \tau_w)^{n_w - 1} \cdot (1 - \tau_l)^{n_l}. \tag{15}$$

Similarly, the collision probability for an LTE-LAA eNB with at least one of the other remaining $(n_l - 1)$ eNBs and n_w Wi-Fi APs can be given by:

$$P_l = 1 - (1 - \tau_l)^{n_l - 1} \cdot (1 - \tau_w)^{n_w}. \tag{16}$$

We can now solve (11), (14), (15) and (16) jointly using numerical methods to compute the values of P_w, P_l, τ_w, and τ_l.

The transmission Probability of a Wi-Fi AP under this heterogeneous setup is the probability that at least one of the n_w

APs transmit a packet during a time slot. This can be given by the probability:

$$P_{trw} = 1 - (1 - \tau_w)^{n_w}. \quad (17)$$

Similarly, the transmission Probability of an LTE-LAA eNB is the probability that at least one of the n_l eNBs transmit during a time slot. This probability can be given by:

$$P_{trl} = 1 - (1 - \tau_l)^{n_l}. \quad (18)$$

Using (17) and (18) we can now express the probability of successful transmission per station type. For Wi-Fi, the probability of successful transmission is the probability that exactly one of the n_w Wi-Fi APs and non of the n_l LTE-LAA eNBs makes a transmission attempt in a given time slot. This can be expressed as:

$$P_{sw} = \frac{n_w \tau_w (1 - \tau_w)^{n_w - 1}(1 - \tau_l)^{n_l}}{P_{trw}}. \quad (19)$$

Similarly, the probability of successful transmission of an LTE-LAA node is the probability that exactly one of the n_l eNBs and non of the n_w Wi-Fi stations makes a transmission attempt in a given time slot. This can be expressed as:

$$P_{sl} = \frac{n_l \tau_l (1 - \tau_l)^{n_l - 1}(1 - \tau_w)^{n_w}}{P_{trl}}. \quad (20)$$

LTE and Wi-Fi use different modulation and coding schemes (MCS). In addition, in the coexistence scenario, eNBs and APs will change their MCS adaptively according to the channel state information, so their transmission rate will be dynamic. Assessing coexistence fairness by including system specific achievable bitrate, introduces an imbalance between the actual channel usage time of the two systems, and therefore results in imprecise interpretation of coexistence fairness. Assessing modulation or coding efficiency of both systems is not the subject and beyond the scope of this work. Therefore, to realize fairness of channel occupancy between the two systems, we assume both have equal bitrate, and express the saturation throughput in terms of the ratio of successful transmission time to the total channel time. Thus, we assume that both systems have equal efficiency when capturing the channel. We can now express the saturation throughput for Wi-Fi as:

$$T_{put_w} = \frac{P_{trw} P_{sw} D_w}{T_{state}}, \quad (21)$$

and the saturation throughput of LAA can be expressed as:

$$T_{put_l} = \frac{P_{tr} P_{sl} D_l}{T_{state}}. \quad (22)$$

Here $D_w = \frac{PacketSize}{Bitrate}$. $D_l = T_{mcot,p}$. T_{state} is the normalizing condition which accounts for every possible scenario that can occur over the channel.

$$\begin{aligned} Tstate = {} & (1 - P_{trw})(1 - P_{trl})\sigma \\ & +...P_{trw} P_{sw}(1 - P_{trl}) T_{ws} \\ & +...P_{trl} P_{sl}(1 - P_{trw}) T_{ls} \\ & +...P_{trw}(1 - P_{sw})(1 - P_{trl}) T_{wc} \\ & +...P_{trl}(1 - P_{sl})(1 - P_{trw}) T_{lc} \\ & +...P_{trw} P_{sw} P_{trl} P_{sl} T_a \\ & +...P_{trw} P_{sw} P_{trl}(1 - P_{sl}) T_a \\ & +...P_{trw}(1 - P_{sw}) P_{trl} P_{sl} T_a \\ & +....P_{trw}(1 - P_{sw}) P_{trl}(1 - P_{sl}) T_a. \end{aligned}$$

σ is the time slot duration. T_{ws} is the duration of time the channel was sensed busy due to a successful transmission of Wi-Fi. T_{ls} is the duration of time the channel was sensed busy due to a successful transmission of LTE-LAA. T_{wc} is the duration of time the channel was sensed busy due to a collision transmission of Wi-Fi. T_{lc} is the duration of time the channel was sensed busy due to a collision transmission of LTE-LAA. T_a is the duration of time the channel was sensed busy due to an inter-network transmission between Wi-Fi and LTE-LAA and is given as the larger timer between both.

The following subsections will explore the coexistence performance under both network scenarios. However, to obtain a greater understanding of the coexistence performance of the underlying LBT mechanism of LTE-LAA, subsection (A) will analyze coexistence performance by setting equal parameter values to both network types. This follows the same thought process developed in section 5A during performance analysis. The objective is to once more isolate the effect of all parameters except the underlining LBT mechanism in operation under heterogeneous co-channel mode, which allows us to identify the affect of the standardized LBT mechanism itself on the performance metric investigated. After that, subsection (B) proceeds to perform the analysis using standard specified parameters for each system, exploring different priority classes defined in the standard, and depicting the coexistence performance of each system. Finally, we show cases where an LTE-LAA eNBs gains an advantage over Wi-Fi co-located and co-channeling stations.

A. EQUAL PARAMETER COEXISTENCE FOR LTE-LAA AND WI-FI

For equations (21) and (22), T_{state} contains the timers for a successful transmission and collision events. For Wi-Fi these expressions can be given as:

$$T_{wc} = (H + EP)/b_r + \delta + DIFS \quad (23)$$

$$T_{ws} = (H + EP)/b_r + \delta + SIFS + ACK + \delta + DIFS \quad (24)$$

For this section we assume LTE-LAA utilizes the same timer durations as Wi-Fi (i.e. $T_{wc} = T_{lc}$ and $T_{ws} = T_{ls}$). The parameters values of equations (23) and (24) are listed in table 5. Figure 6 illustrates the total normalized saturation throughput, and the throughput achieved per network type. The number of heterogeneous nodes per network type are equal to half the number of nodes listed in the x-axis. i.e. $n_l = n_w = n/2$. We observe that the total sum channel utilization throughput of the heterogeneous network is higher than a homogeneous network consisting of the same number of LTE-LAA eNBs (i.e. throughput 20eNBs + 20APs > throughput 40 eNBs).

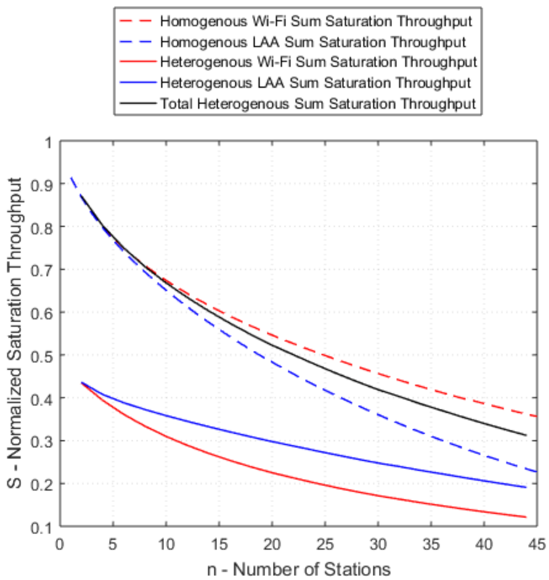

FIGURE 6. **Normalized saturation throughput for an equal parameter heterogeneous network.**

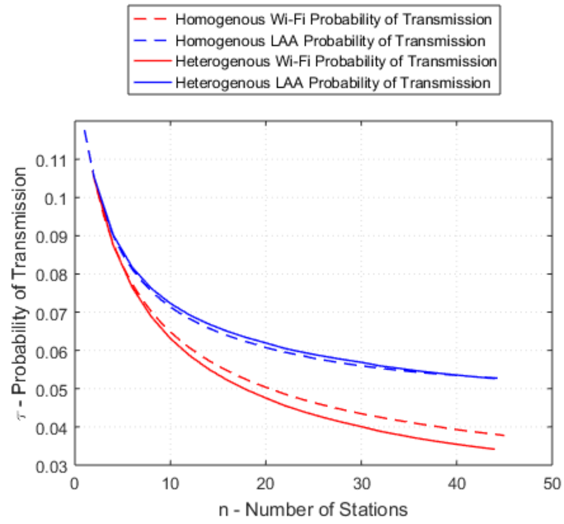

FIGURE 7. **Probability of transmission for an equal parameter heterogeneous network.**

TABLE 5. **Channel access parameters for coexistence study.**

Parameter	Unit
m_p	2
$CW_{p,min}$:	15
$T_{mcot,p}$: Maximum channel occupancy time	8ms
EP: Packet Payload	8kbits
br: bitrate	1Mbps
δ: Propagation Delay	$1\mu s$
H: Packet Header (PHY + MAC)	400bits
ACK: HARQ-ACK	240bits
σ: TimeSlot	$9\mu s$
DIFS:	$34\mu s$
T_d:	$16\mu s + (m_p + \sigma)$
SIFS	$16\mu s$
K Parameter	1

This can be attributed to the increasing collisions that occur in a dense homogeneous LTE-LAA network when K=1. However, we also observe the total throughput of the heterogeneous LTE-LAA network exceeds that of Wi-Fi as the number of nodes increases. This occurs due to the increase in collisions occurring. For this, Wi-Fi retains a higher backoff stage increasing its backoff time, while LAA resets to a lower stage which results in an increased opportunity of capturing the channel and transmitting. This aligns with insights attained from the performance analysis part shown in section 5A. Furthermore, it can be concluded that the LBT mechanism of LTE-LAA does provide an advantage over Wi-Fi when all other parameters are equal. Results are confirmed when we observe figure 7 illustrating the probability of transmission for both networks in heterogeneous operation. We see that LTE-LAA's transmission probability marginally increases above the homogeneous network case, whereas Wi-Fi's transmission probability somewhat decreases below its homogeneous counterpart. Nevertheless, in all cases, LTE-LAA retains a higher transmission probability over Wi-Fi.

B. STANDARDIZED PARAMETER COEXISTENCE FOR LTE-LAA AND WI-FI

In this subsection we conduct heterogeneous coexistence analysis under standard specified parameter settings for each network. However, for this analysis to be complete, we note the following considerations, characteristic of LTE-LAA, which are taken into account in the analysis: 1) Upon completing the channel access procedures and capturing the channel, the eNB can continuously transmit on a carrier on which the LAA Scell transmissions are to be performed for $t_{mcot,p}$ as shown in table 1 for each priority class. This transmission opportunity can be up to 8ms for priority class 4, and 10ms if the absence of any other technology sharing the carrier can be guaranteed on a long term basis (e.g. by level of regulation). Therefore, under saturation and ideal channel conditions assumed, the eNB will utilize its full transmission opportunity. 2) A new frame structure type 3 is applicable to LAA. Each radio frame is 10 ms long and consists of 10 subframes of length 1 ms. Any of these 10 subframes can be used for uplink/downlink transmission or can be empty. LAA transmission can start and end at any subframe and can consist of one or more consecutive subframes in the burst. LAA downlink transmission can start from the 0th Orthogonal Frequency Division Multiplexing (OFDM) symbol (Subframe boundary) or from the 7th OFDM symbol (Second Slot Starting Position) of a subframe. LAA downlink transmission can either end at the subframe boundary or at any of the Downlink Pilot Time Slot (DwPTS) symbols. Therefore, the last subframe can be completely occupied with 14 OFDM symbols or can consist of any of DwPTS duration symbols. Figure 8 depicts this new frame structure type 3, the slot boundaries and DwPTS duration symbols. 3) Once transmission is complete, the receiver transmits the acknowledgment through the licensed band if the symbols are successfully decoded. A reference subframe which is

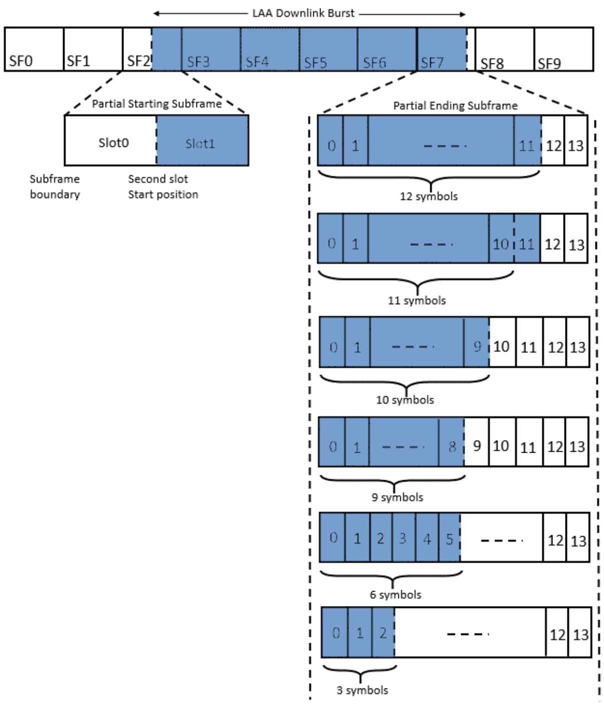

FIGURE 8. LTE-LAA frame 3 structure.

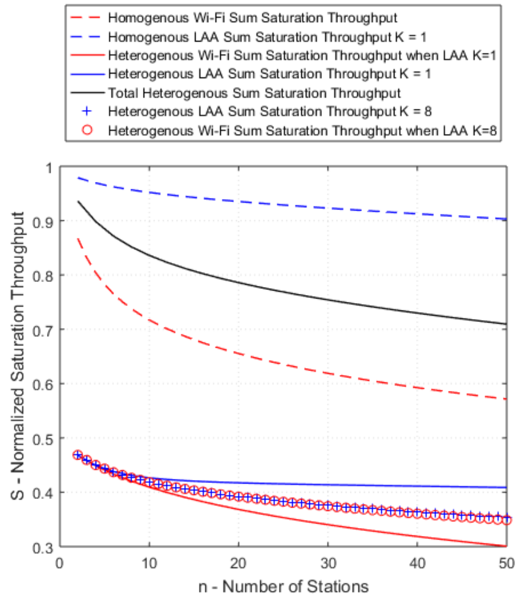

FIGURE 9. Priority = 4, m_p = 7, m_{wifi} = 7 and contention window steps W ∈ [15,31,63,127,255,511,1023].

the starting subframe of the most recent transmission on the carrier made by the eNB, for which at least some HARQ-ACK feedback is expected to be available is considered for assessing retransmissions. Thus, the minimum resolution of a data re-transmission and the collision time in LTE-LAA is one sub frame. With the assumption of saturation and ideal channel conditions, an upper boundary can be set for the number of subframes transmitted. (e.g. the maximum number of subframes that can be transmitted for priority class 4 is 8 sub frames, each 1ms). Therefore, when an LTE-LAA eNB captures and successfully transmits, the duration of time the channel is sensed busy can be expressed as:

$$T_{ls} = T_{mcot,p} + \delta + T_d \tag{25}$$

$T_{mcot,p}$ is the TxOP of the LTE-LAA (8ms for p=4). This indicates that once the eNB captures the channel, it will saturate the channel for the total amount of time ($T_{mcot,p}$) that it is allowed. T_d is the standard specified sensing time equivelent to DIFS for Wi-Fi. δ and T_d can be found in table 5. The duration of time the channel is sensed busy when an LTE-LAA eNB transmission experiences collision under saturation and ideal channel conditions is expressed as:

$$T_{lc} = T_{subframe} + \delta + T_d \tag{26}$$

$T_{subframe} = 1ms$.

Using the above derived expressions, we proceed to analyze different coexistence cases pertaining to different priority classes as defined in the standard.

For priority class $p = 4$, the standard defines contention window steps W ∈ [15,31,63,127,255,511,1023], number of contention stages $m_p = 7$, and transmission opportunity duration of $T_{mcot,p} = 8ms$. Figure 9 depicts coexistence performance results attained for this priority class. We first observe that under standardized parameters, the saturation throughput of homogeneous coexistence operation achieved in LTE-LAA eNBs is comparatively higher than that of Wi-Fi APs for all network densities. This is attributed to two factors: 1) The use of the licensed band for sending HAQR-ACK messages which allows for increased channel utilization of the unlicensed band. 2) The increased efficiency attained from the larger successful transmission time opposed to the reduced collision time occurring over the minimum resolution time of LTE-LAA. However, this performance difference between LTE-LAA and Wi-Fi at smaller node numbers disappears under the heterogeneous network scenario. This occurs because the collision time increases to that of the higher of both networks, as can be seen in the T_{state} expression found in equation (21) and (22). At the same time and despite the unfavorable effect of Wi-Fi's collision time on channel utilization, we observe that LTE-LAA continually achieves increasing throughput as the number of nodes in the system increases. This occurs because of the LAA LBT mechanism confirming the insights found in section 5A. As the number of nodes increases, the number of collisions increases, which causes Wi-Fi APs to retransmit at the higher stages, whereas LAA eNBs reset gaining an increased transmission opportunity. We also observe in figure 9 that the total heterogeneous sum saturation throughput of the system is higher than homogeneous Wi-Fi, which occurs due to LTE-LAA's increased channel utilization and efficiency. Finally, we observe in figure 9 that by setting K=8, the saturation throughput and performance of LTE-LAA almost matches Wi-Fi to a negligible difference confirming the insights obtained in the

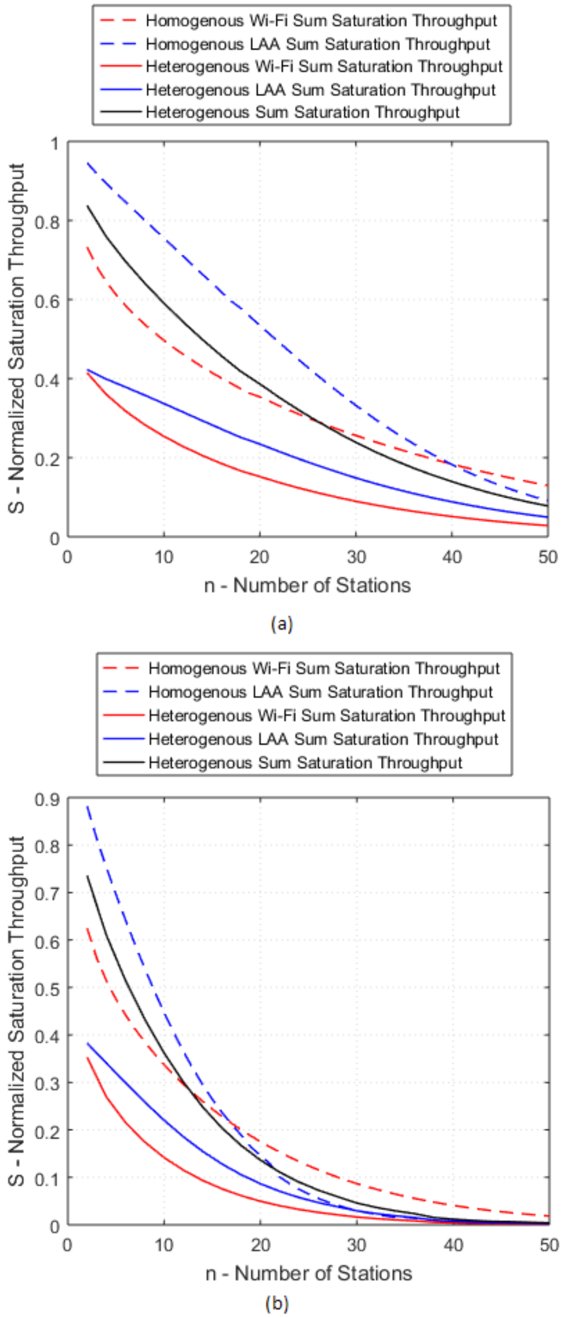

FIGURE 10. a) Priority = 2, $m_p = 1$, $m_{wifi} = 1$ and W ∈ [7,15]. b) Priority = 1, $m_p = 1$, $m_{wifi} = 1$ and W ∈ [3,7].

performance analysis of the LBT mechanism presented section 5A.

For priority class $p = 2$, the standard defines W ∈ [7,15], $m_p = 1$, and $T_{mcot,p} = 3ms$ and for priority class $p = 1$, the standard defines W ∈ [3,7], $m_p = 1$, and $T_{mcot,p} = 2ms$. Figure 10 (a) and (b) depict the results attained for $p = 2$ and $p = 1$ respectively. We observe that LTE-LAA saturation throughput converges towards Wi-Fi's throughput in contrast to the diverging behaviour we observed for priority class 4.

This is the result of a dual affect caused by the small contention window sizes and backoff stages for these priority classes. As the number of nodes increases, the higher saturation throughput attained from the increased transmission probability diminishes as a result of the increasing collisions occurring. We observe that even for a homogenous network, for priority 2, and around $n = 40$, the saturation throughput drops below that of Wi-Fi gradually lowering the improved channel utilization and efficiency that LTE-LAA was achieving over Wi-Fi. Likewise, we find this threshold dropping further for Priority $P = 1$, to around $n = 17$.

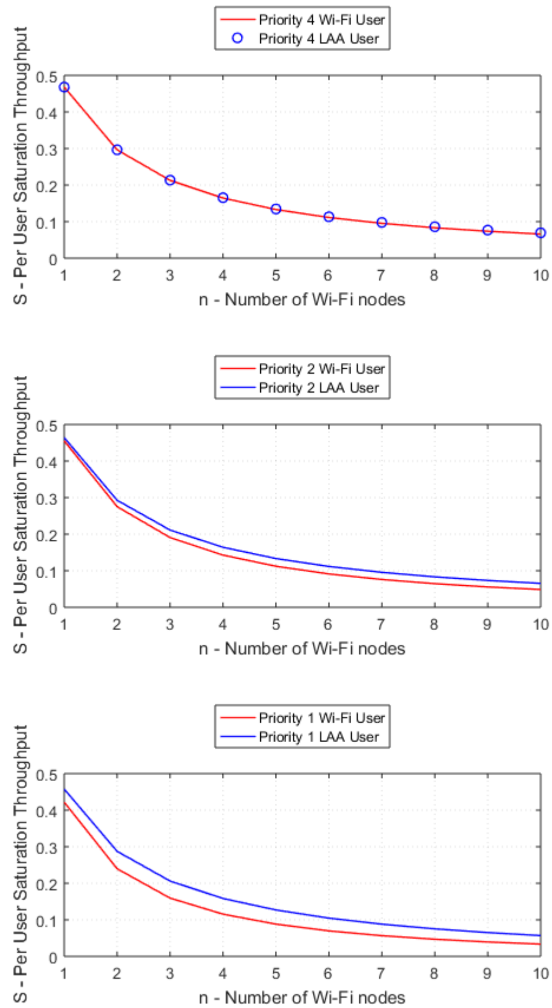

FIGURE 11. Individual User Saturation Throughput for Priority Class P = {4, 2, 1}.

Finally, to illustrate the gain a single LAA user achieves over incumbant Wi-Fi stations when operating under co-channel heterogeneous mode, we consider a scenario where one LAA eNB is amongst (n) Wi-Fi AP stations. By dividing the total sum saturation throughput per network type over the number of nodes, we compute the saturation throughput per network station. Figure 11 depicts the results attained. We observe for priority class 4, that the saturation throughput of an LTE-LAA station closely follows that of Wi-Fi regardless of the number of Wi-Fi nodes present. This is due to the large backoff stages, low density of nodes present and low number of retransmissions occurring, resulting in an insignificant difference in performance. However, we observe for priority class 1 and 2, that an LTE-LAA station achieves slightly higher saturation throughput than Wi-Fi. This continually occurs despite the increasing number of Wi-Fi nodes present in the network. Therefore, we find that under the more commonly found low density heterogeneous networks, an LTE-LAA station achieves similar performance to Wi-Fi for priority class 4, and attains an advantage for higher priority classes (1,2 and 3).

VII. CONCLUSION

In this paper, we have proposed and developed a Markov Chain to accurately model the LBT mechanism of LTE-LAA 3GPP release 13 and 14. The proposed model also applies to the Multefire specification which has adopted the LTE-LAA LBT mechanism. Model validation was demonstrated through numerical and simulation analysis. By means of the proposed model, performance evaluation of the standardized LAA-LBT was examined. Results indicate LTE-LAA LBT achieves higher probability of transmission compared to Wi-Fi LBT. Furthermore, a comprehensive coexistence analysis of both homogenous and heterogenous network scenarios was examined. Results indicate LAA achieves increased throughput over Wi-Fi as the number of nodes operating the channel increases. This developed model serves as an analytical tool that allows numerical analysis of the current standardized LTE-LAA with any future enhancements.

DISCLAIMER

The mention of commercial products, their sources, or their use in connection with material reported herein is not to be construed as either an actual or implied endorsement of such products by the Department of Health and Human Services.

ACKNOWLEDGMENT

This work was supported in part by an appointment to the Internship/Research Participation Program at the U.S. Food and Drug Administration, administered by the Oak Ridge Institute for Science and Education through an inter-agency agreement between the U.S. Department of Energy and the FDA.

REFERENCES

[1] "Cisco visual networking index: Global mobile data traffic forecast update, 2016–2021," Cisco, San Jose, CA, USA, White Paper c11-520862, 2017. [Online]. Available: https://www.cisco.com/c/en/us/solutions/collateral/service-provider/visual-networking-index-vni/mobile-white-paper-c11-520862.pdf

[2] Qualcomm Incorporated. *Extending LTE Advanced to Unlicensed Spectrum*. Accessed: May 2018. [Online]. Available: https://www.qualcomm.com/media/documents/files/white-paper-extending-lte-advanced-to-unlicensed-spectrum.pdf

[3] HUAWEI. *U-LTE: Unlicensed Spectrum Utilization of LTE, 2014*. Accessed: May 2018. [Online]. Available: www.huawei.com/ilink/en/download/HW_327803

[4] Ericsson. *LTE License Assisted Access*. Accessed May 2018. [Online]. Available: https://web.archive.org/web/20161014143936/http://www.ericsson.com/res/thecompany/docs/press/media_kits/ericsson-license-assisted-access-laa-january-2015.pdf

[5] Qualcomm Incorporated. *Introducing Multefire: LTE-Like Performance With Wi-Fi Like Simplicity*. Accessed: May 2018. [Online]. Available: https://www.qualcomm.com/news/onq/2015/06/11/introducing-multefire-lte-performance-wi-fi-simplicity

[6] N. Rupasinghe and I. Güvenç, "Licensed-assisted access for WiFi-LTE coexistence in the unlicensed spectrum," in *Proc. IEEE Globecom Workshops (GC Wkshps)*, Austin, TX, USA, Dec. 2014, pp. 894–899.

[7] Y. Jian, C.-F. Shih, B. Krishnaswamy, and R. Sivakumar, "Coexistence of Wi-Fi and LAA-LTE: Experimental evaluation, analysis and insights," in *Proc. IEEE Int. Conf. Commun. Workshop (ICCW)*, London, U.K., Jun. 2015, pp. 2325–2331.

[8] S. Xu, Y. Li, Y. Gao, Y. Liu, and H. Gačanin, "Opportunistic coexistence of LTE and WiFi for future 5G system: Experimental performance evaluation and analysis," *IEEE Access*, vol. 6, pp. 8725–8741, 2018.

[9] A. M. Cavalcante, "Performance evaluation of LTE and Wi-Fi coexistence in unlicensed bands," in *Proc. IEEE 77th Veh. Technol. Conf. (VTC Spring)*, Dresden, Germany, Jun. 2013, pp. 1–6.

[10] T. Nihtilä *et al.*, "System performance of LTE and IEEE 802.11 coexisting on a shared frequency band," in *Proc. IEEE Wireless Commun. Netw. Conf. (WCNC)*, Shanghai, China, Apr. 2013, pp. 1038–1043.

[11] F. M. Abinader *et al.*, "Enabling the coexistence of LTE and Wi-Fi in unlicensed bands," *IEEE Commun. Mag.*, vol. 52, no. 11, pp. 54–61, Nov. 2014.

[12] *LTE-U Forum*. Accessed: May 2018. [Online]. Available: https://web.archive.org/web/20170316191518/ and http://www.lteuforum.org/

[13] "LTE in unlicensed spectrum: Harmonious coexistence with Wi-Fi," Qualcomm Res., San Jose, CA, USA, White Paper, 2012. [Online]. Available: https://www.qualcomm.com/media/documents/files/lte-unlicensed-coexistence-whitepaper.pdf

[14] A. Mukherjee *et al.*, "System architecture and coexistence evaluation of licensed-assisted access LTE with IEEE 802.11," in *Proc. IEEE Int. Conf. Commun. Workshop (ICCW)*, Jun. 2015, pp. 2350–2355.

[15] Y. Song, K. W. Sung, and Y. Han, "Coexistence of Wi-Fi and cellular with listen-before-talk in unlicensed spectru," *IEEE Commun. Lett.*, vol. 20, no. 1, pp. 161–164, Jan. 2016.

[16] C. Chen, R. Ratasuk, and A. Ghosh, "Downlink performance analysis of LTE and WiFi coexistence in unlicensed bands with a simple listen-before-talk scheme," in *Proc. IEEE 81st Veh. Technol. Conf. (VTC Spring)*, Glasgow, Scotland, May 2015, pp. 1–5.

[17] R. Yin, G. Yu, A. Maaref, and G. Y. Li, "Adaptive LBT for licensed assisted access LTE networks," in *Proc. IEEE GLOBECOM*, San Diego, CA, USA, Dec. 2015, pp. 1–6.

[18] S. Saadat, D. Chen, K. Luo, M. Feng, and T. Jiang, "License assisted access-WiFi coexistence with TXOP backoff for LTE in unlicensed band," *China Commun.*, vol. 14, no. 3, pp. 1–14, Mar. 2017.

[19] Y. Li, T. Zhou, Y. Yang, H. Hu, and M. Hamalainen, "Fair downlink traffic management for hybrid LAA-LTE/Wi-Fi networks," *IEEE Access*, vol. 5, pp. 7031–7041, 2017.

[20] T. Tao, F. Han, and Y. Liu, "Enhanced LBT algorithm for LTE-LAA in unlicensed band," in *Proc. IEEE 26th Annu. Int. Symp. Pers., Indoor, Mobile Radio Commun. (PIMRC)*, Hong Kong, Aug./Sep. 2015, pp. 1907–1911.

[21] V. Mushunuri, B. Panigrahi, H. K. Rath, and A. Simha, "Fair and efficient listen before talk (LBT) technique for LTE licensed assisted access (LAA) networks," in *Proc. IEEE 31st Int. Conf. Adv. Inf. Netw. Appl. (AINA)*, Taipei, Taiwan, Mar. 2017, pp. 39–45.

[22] J. Wang, J. Du, J. Xu, and H. Wu, "Harmonious coexistence solution between stand-alone LTE and WiFi in unlicensed band," *Trans Emerg. Telcommun. Tech.*, vol. 28, no. 9, p. e3155, 2017, doi: 10.1002/ett.3155.

[23] A. Bhorkar, C. Ibars, A. Papathanassiou, and P. Zong, "Medium access design for LTE in unlicensed band," in *Proc. IEEE Wireless Commun. Netw. Conf. Workshops (WCNCW)*, New Orleans, LA, USA, Mar. 2015, pp. 369–373.

[24] H. Wang, M. Kuusela, C. Rosa, and A. Sorri, "Enabling frequency reuse for licensed-assisted access with listen-before-talk in unlicensed bands," in *Proc. IEEE VTC Spring*, Nanjing, China, May 2016, pp. 1–5.

[25] Q. Chen, G. Yu, A. Maaref, Y. Li, and A. Huang, "Rethinking mobile data offloading for LTE in unlicensed spectrum," *IEEE Trans. Wireless Commun.*, vol. 15, no. 7, pp. 4987–5000, Jul. 2016.

[26] *Study on Licensed-Assisted Access to Unlicensed Spectrum*, document TR 36.889 V13.0.0, 3GPP, Jun. 2015.

[27] H.-J. Kwon *et al.*, "Licensed-assisted access to unlicensed spectrum in LTE release 13," *IEEE Commun. Mag.*, vol. 55, no. 2, pp. 201–207, Feb. 2017, doi: 10.1109/MCOM.2016.1500698CM.

[28] Q. Cui, Y. Gu, W. Ni, and R. P. Liu, "Effective capacity of licensed-assisted access in unlicensed spectrum for 5G: From theory to application," *IEEE J. Sel. Areas Commun.*, vol. 35, no. 8, pp. 1754–1767, Aug. 2017.
[29] J. Yi, W. Sun, S. Park, and S. Choi, "Performance analysis of LTE-LAA network," *IEEE Commun. Lett.*, vol. 22, no. 6, pp. 1236–1239, Jun. 2018, doi: 10.1109/LCOMM.2017.2779752.
[30] J. Zhang, M. Wang, M. Hua, T. Xia, W. Yang, and X. You, "LTE on license-exempt spectrum," *IEEE Commun. Surveys Tuts.*, vol. 20, no. 1, pp. 647–673, 1st Quart., 2018.
[31] *Evolved Universal Terrestrial Radio Access (E-UTRA) Physical Layer Procedures*, document TS 36.213 V13.6.0, 3GPP, Jun. 2017.
[32] S. Wang, Q. Cui, and Y. Gu, "Performance analysis of multi-carrier LAA and Wi-Fi coexistence in unlicensed spectrum," in *Proc. IEEE/CIC Int. Conf. Commun. China (ICCC)*, Qingdao, China, Oct. 2017, pp. 1–5.
[33] Y. Zhang, Y. Chang, and T. Zeng, "Coexistence performance analysis of LAA based on release 13," in *Proc. Int. Symp. Wireless Commun. Syst. (ISWCS)*, Bologna, Italy, Aug. 2017, pp. 90–95.
[34] O. El-Samadisy, M. Khedr, and A. El-Helw, "Performance evaluation of MAC for IEEE 802.11 and LAA LTE," in *Proc. Int. Conf. Comput. Sci. Comput. Intell. (CSCI)*, Las Vegas, NV, USA, Dec. 2016, pp. 923–928.
[35] Y. Gao, Q. Huang, S. Xu, H. Li, Z. Li, and W. Tang, "Experimental performance evaluation and analysis of LAA and Wi-Fi coexistence in the unlicensed spectrum," in *Proc. IEEE Globecom Workshops (GC Wkshps)*, Washington, DC, USA, Dec. 2016, pp. 1–6.
[36] Y. Gao, X. Chu, and J. Zhang, "Performance analysis of LAA and WiFi coexistence in unlicensed spectrum based on Markov chain," in *Proc. IEEE Global Commun. Conf. (GLOBECOM)*, Washington, DC, USA, Dec. 2016, pp. 1–6.
[37] X. Yan, H. Tian, and C. Qin, "A Markov-based modelling with dynamic contention window adaptation for LAA and WiFi coexistence," in *Proc. IEEE 85th Veh. Technol. Conf. (VTC Spring)*, Sydney, NSW, Australia, Jun. 2017, pp. 1–6.
[38] Z. Tang, X. Zhou, Q. Hu, and G. Yu, "Throughput analysis of LAA and Wi-Fi coexistence network with asynchronous channel access," *IEEE Access*, vol. 6, pp. 9218–9226, 2018.
[39] M. Mehrnoush, V. Sathya, S. Roy, and M. Ghosh. (2018). "Analytical modeling of Wi-Fi and LTE-LAA coexistence: Throughput and impact of energy detection threshold." [Online]. Available: https://arxiv.org/abs/1803.02444
[40] *IEEE Standard for Information Technology—Telecommunications and Information Exchange Between Systems Local and Metropolitan Area Networks—Specific Requirements—Part 11: Wireless LAN Medium Access Control (MAC) and Physical Layer (PHY) Specifications*, IEEE Standard 802.11-2016, (Revision of IEEE Std 802.11-2012), Dec. 2016, pp. 1–3534.
[41] *Multi-Node Tests for Licence-Assisted Access (LAA)*, document TR 36.789 V13.0.0, 3GPP, Jun. 2017.
[42] *Evolved Universal Terrestrial Radio Access (E-UTRA) and Evolved Universal Terrestrial Radio Access Network (E-UTRAN); Overall description*, document TS 36.300 V13.8.0, 3GPP, Jun. 2017.
[43] *Physical Channels and Modulation*, document TS 36.211 V13.6.0, 3GPP, Jun. 2017.
[44] *Base Station (BS) Radio Transmission and Reception*, document TS 36.104 V13.8.0, 3GPP, Jun. 2017.
[45] *Base Station (BS) Conformance Testing*, document TS 36.141 V13.8.0, 3GPP, Jun. 2017.
[46] *Requirements for Support of Radio Resource Management*, document TS 36.133 V13.8.0, 3GPP, Jun. 2017.
[47] *QoS Class Identifier*. Accessed: May 2018. [Online]. Available: https://en.wikipedia.org/wiki/QoS_Class_Identifier
[48] G. Bianchi, "Performance analysis of the IEEE 802.11 distributed coordination function," *IEEE J. Sel. Areas Commun.*, vol. 18, no. 3, pp. 535–547, Mar. 2000.
[49] M. Ergen and P. Varaiya, "Throughput analysis and admission control for IEEE 802.11a," *Mobile Netw. Appl.*, vol. 10, no. 5, pp. 705–716, 2005.

NAIM BITAR (S'14) received the B.Sc. degree in telecommunication engineering in 2010, the M.Sc. degree in electrical and computer engineering from The University of Oklahoma (OU), Norman, OK, USA, in 2016, where he is currently pursuing the Ph.D. degree. He is currently a Research Assistant with the Wireless and Electromagnetic Compliance and Design Center, OU. His research interests include modeling and coexistence performance analysis of wireless and mobile communication systems, data analytics, data mining, engineering optimization, machine learning, and its applications in wireless and mobile networks.

MOHAMAD OMAR AL KALAA (M'18) received the bachelor's degree from Damascus University, Damascus, Syria, in 2008, the M.E. degree from TELECOM Bretagne in 2012, and the M.Sc. and Ph.D. degrees from The University of Oklahoma, Norman, OK, USA, in 2014 and 2016, respectively. He is currently a Staff Fellow and an Electrical Engineer with the Center for Devices and Radiological Health, U.S. Food and Drug Administration. His research interests include wireless coexistence of technologies in unlicensed bands, coexistence testing methodologies, cognitive radio, PHY and MAC design, and the applications of machine learning in wireless communication.

SETH J. SEIDMAN (M'06) received the bachelor's and master's degrees in electrical engineering from the University of Maryland. He is currently a Research Electrical Engineer with 15 years' of experience with the U.S. Food and Drug Administration. He performs regulatory reviews, research, and has authored papers in the areas of medical device EMC and wireless coexistence. He is also a U.S. representative to International Standards Organization and International Electrotechnical Commission Joint Technical Committee 1, Subcommittee 31 on automatic identification and data capture techniques, an FDA representative to the Association for Automatic Identification and Mobility, a Co-Chairman to the Association for the Advancement of Medical Instrumentation EMC Committee for Pacemakers and ICDs, and a Vice Chair to the American National Standards Institute C63 Subcommittee 7 on Spectrum Etiquette.

HAZEM H. REFAI (M'92) is currently the Williams Chair of telecommunication and networking with the School of Electrical and Computer Engineering Telecommunication Program, The University of Oklahoma (OU), Tulsa, OK, USA. He is also the Founder and the Director of the Wireless Electromagnetic Compliance and Design (WECAD) Center, OU. WECAD's mission is to conduct basic and applied research examining wireless coexistence. He has published over 190 referred papers for national and international conferences and Journal articles. His fields of interest include the development of optical wireless communication, physical and medium access control layers to enhance wireless coexistence, and cognitive radios and networks. He is a past IEEE ComSoc Tulsa Chapter President and served as the organization's North American Distinguished Lecturer Tour Coordinator.